Vibrational Dynamics of the Neutral Naphthalene Molecule from a Tight-Binding Approach

Nguyen-Thi Van-Oanh, Pascal Parneix,* and Philippe Bréchignac

Laboratoire de Photophysique Moléculaire,† C.N.R.S. Bât 210, Université Paris-Sud, F91405 Orsay Cedex, France

Received: June 6, 2002; In Final Form: June 26, 2002

The static and dynamical properties of the neutral naphthalene molecule in its ground electronic state have been investigated using a tight-binding potential. This semiempirical method has allowed us to obtain static information concerning geometry and normal-mode frequencies. Tight-binding molecular dynamics coupled with an adiabatic switching procedure has also given information on the anharmonicity of the potential energy surface of such neutral aromatic molecule. Finally, the absorption spectrum of the neutral naphthalene molecule, prepared in its ground vibrational state, has been calculated from the Fourier transform of the dipole autocorrelation function and compared with the experimental data.

I. Introduction

In the middle of the 1980s, two groups[1−5] independently proposed that polycyclic aromatic hydrocarbons (PAH) molecules could be responsible for the characteristic infrared emission spectrum first observed by Russell et al.[6,7] These infrared bands called "unidentified infrared bands" (UIB), observed systematically from the different regions of interstellar space, which are heated by starlight, present a spectroscopic correspondence with the typical C−C and C−H bands in the aromatic molecules (the most intense UIBs appear at $\lambda = 3.3$, 6.2, 7.7, 8.6, and 11.3 μm).

Free PAH molecules do possess the adequate photophysical properties[1−5] to allow for the transient heating mechanism proposed by Sellgren[8] to account for the strength of the short wavelength band. In this scheme, a PAH molecule flying freely in space absorbs an UV photon, emitted by the stellar radiation field, which induces an electronic transition. Because of the strong coupling between the electronic and vibrational degrees of freedom (fast internal conversion) in such a large molecule, the molecular system is rapidly (subpicosecond time scale) transferred to a lower electronic state with a larger amount of vibrational energy. Then, the two only ways for an isolated molecule to be cooled are the radiative vibrational emission and the fragmentation. The evaluation of the relative yields of these two channels is a difficult task and the understanding of the dynamics of highly vibrationally excited molecules appears as a challenge for experimentalists as well as for theoreticians.

In the theoretical work presented here, we focus our study of the absorption infrared spectrum on the smallest PAH molecule, i.e., the $C_{10}H_8$ neutral naphthalene. Most of the experimental data have been collected using the matrix isolation technique, which gives spectroscopic information on the cold neutral naphthalene.[9,10] The main difficulty of this technique comes from the fact that the molecules are not isolated and are interacting with the rare-gas matrix. Spectroscopic data can be slightly modified by the local environment. Some vibrational shifts and homogeneous (coupling between the intramolecular modes and the phonon modes) and inhomogeneous broadenings (vibrational shifts can depend on the molecular site inside the matrix) can thus be induced in such experiments.

From the theoretical point of view, some ab initio calculations of the $C_{10}H_8$ system have been performed first by Pauzat et al.[11] (Hartree−Fock (HF) calculations) and then by Langhoff[12] and Martin et al.[13] (density functional theory (DFT)). All of these analyses are developed using the harmonic approximation (normal-mode analysis). On the other hand, the molecules are expected to be highly vibrationally excited in the astrophysical context. Therefore, we have developed a theoretical approach able to deal with such excited states. A tight-binding molecular dynamics (TBMD) simulation of hybrid covalent carbon−hydrogen systems, combined with the semiclassical adiabatic switching technique allowing us to obtain the initial configurations at given values of the total energy, can be used to obtain the IR spectra of large PAHs as a function of the vibrational temperature. In this article, we present the technique and then apply it to naphthalene in its ground vibrational state (at $T = 0$ K).

II. Potential Energy Surface and Methodology

A. Tight-Binding Potential. We describe here the tight-binding (TB) approach which has been used to build the potential energy surface (PES). The main advantage of this method is to incorporate electronic effects using a semiempirical potential calculated with a minimal atomic basis. The quantum-mechanical nature of the covalent bonds is directly taken into account in the electronic structure evaluated at each time step of the propagation of the classical equations. Consequently, the multiatom nature of the interaction in a covalent system is also taken into account. As the dynamics of the electrons are not explicitly solved, the time step of the integration of the classical motions is only imposed by the nuclear motions (about 0.1 fs). This important feature allows us to simulate the dynamics of large systems which cannot be treated by much more sophisticated methods such as the Car−Parinello method[14] in which the time-step for integration is considerably smaller. The TB semiempirical approach has been widely used to study anharmonic effects in solids[15] but also to describe static and dynamical properties in liquids[16] and clusters.[17,18]

To our knowledge, two sets of TB parameters for the mixed carbon−hydrogen systems[19,20] can be found in the literature. These parameters have been fitted on the static properties (geometry of the molecule) and on the normal-mode frequencies

* To whom correspondence should be addressed.
† Laboratoire associé à l'Université Paris-Sud.

10.1021/jp026250e CCC: $22.00 © 2002 American Chemical Society
Published on Web 09/28/2002

TABLE 1: Empirical Tight-Binding Parameters for the C−H and H−H Interaction[a]

TB parameters	set (I)	set (II)	set (III)	TB parameters	set (I)	set (II)	set (III)
C−H interaction				H−H interaction			
$r_0^{(C-H)}$ (Å)	1.09	1.094	1.047	$r_0^{(H-H)}$ (Å)		0.742	0.742
$t_{ss\sigma}^{(C-H)}$ (eV)	−6.9986	−4.81	−6.6989	$t_{ss\sigma}^{(H-H)}$ (eV)		−6.374	−6.374
$t_{sp\sigma}^{(C-H)}$ (eV)	7.390	5.32	7.37	$V_{core}^{(H-H)}$ (eV)		8.0	8.0
$V_{core}^{(C-H)}$ (eV)	10.8647	7.923	11.1294	$n_a^{(H-H)}$ for $t_{ss\sigma}^{(H-H)}$		1.59	1.59
$n_a^{(C-H)}$ for $t_{ss\sigma}^{(C-H)}$	1.970	1.949	1.971	$m_a^{(H-H)}$		2.52	2.52
$n_a^{(C-H)}$ for $t_{sp\sigma}^{(C-H)}$	1.603	1.949	1.603	$r_t^{(H-H)}$ (Å)		1.5	1.5
$m_a^{(C-H)}$	3.100	3.372	3.100	$n_c^{(H-H)}$		8.0	8.0
$r_t^{(C-H)}$ (Å)	2.0	2.0	1.98	$n_b^{(H-H)}$ for $t_{ss\sigma}^{(H-H)}$		1.59	1.59
$n_c^{(C-H)}$	9.0	22.0	9.0	$r_c^{(H-H)}$ (Å)		1.5	1.5
$n_b^{(C-H)}$ for $t_{ss\sigma}^{(C-H)}$	1.970	1.949	1.970	$m_c^{(H-H)}$		8.0	8.0
$n_b^{(C-H)}$ for $t_{sp\sigma}^{(C-H)}$	1.603	1.949	1.603	$m_b^{(H-H)}$		2.52	2.52
$r_c^{(C-H)}$ (Å)	1.90	2.0	1.87				
$m_c^{(C-H)}$	10.0	22.0	10.0				
$m_b^{(C-H)}$	3.100	3.372	3.100				

[a] Sets (I) and (II) are quoted from refs 19 and 20. Set (III) is proposed in this work for the aromatic molecules.

TABLE 2: Empirical Tight-Binding Parameters for the C−C Interaction[a]

TB parameters	set (I)	set (II)	set (III)
$\epsilon_s^{(C)}$ (eV)	−10.290	−5.16331	−10.290
$\epsilon_p^{(C)}$ (eV)	0.0	2.2887	0.0
$\epsilon_s^{(H)}$ (eV)	−0.50	0.42583	−0.50
U (eV)	3.0	0.0	3.0
C−C interaction			
$r_0^{(C-C)}$ (Å)	1.312	1.536	1.312
$t_{ss\sigma}^{(C-C)}$ (eV)	−8.42256	−4.43338	−8.77254
$t_{sp\sigma}^{(C-C)}$ (eV)	8.08162	3.78614	8.20162
$t_{pp\sigma}^{(C-C)}$ (eV)	7.75792	5.65984	7.75792
$t_{pp\pi}^{(C-C)}$ (eV)	−3.67510	−1.82861	−3.87510
$V_{core}^{(C-C)}$ (eV)	22.68939	10.92	22.58939
$n_a^{(C-C)}$ for $t_{ss\sigma}^{(C-C)}$	1.29827	2.796	1.29827
$n_a^{(C-C)}$ for $t_{sp\sigma}^{(C-C)}$	0.99055	2.796	0.99055
$n_a^{(C-C)}$ for $t_{pp\sigma}^{(C-C)}$	1.01545	2.796	1.01545
$n_a^{(C-C)}$ for $t_{sp\tau}^{(C-C)}$	1.82460	2.796	1.82460
$m_a^{(C-C)}$	2.72405	4.455	2.62405
$r_t^{(C-C)}$ (Å)	2.00	2.32	2.02
$n_c^{(C-C)}$ for $t_{ss\sigma}^{(C-C)}$, $t_{sp\sigma}^{(C-C)}$, $t_{pp\sigma}^{(C-C)}$, and $t_{pp\sigma}^{(C-C)}$	5.0	22.0	5.0
$n_b^{(C-C)}$ for $t_{ss\sigma}^{(C-C)}$, $t_{sp\sigma}^{(C-C)}$, $t_{pp\sigma}^{(C-C)}$, and $t_{pp\sigma}^{(C-C)}$	1.0	2.796	1.0
$r_c^{(C-C)}$ (Å)	1.9	2.32	1.9
$m_c^{(C-C)}$	7.0	22.0	7.0
$m_b^{(C-C)}$	1.0	4.455	1.0

[a] Sets (I) and (II) are quoted from refs 19 and 20. Set (III) is proposed in this work for the aromatic molecules.

but also on the dissociation energy for systems that involve different hybridizations (sp^1, sp^2, and sp^3).

In the TB formalism, the Hamiltonian is written as

$$H_{TB} = \sum_i \frac{p_i^2}{2m_i} + \sum_i \sum_{j>i} V_{core}^{(i,j)}(r_{ij}) + V_{TB}(\{\mathbf{r}\}) \qquad (1)$$

The first term is the kinetic energy. The second term is the short-range repulsion between the core atoms. This repulsive term has been taken simply as a sum of atom−atom potentials. The analytic form of the repulsive potential between two ions is given by

$$V_{core}^{(i,j)}(r_{ij}) = V_{core}\left(\frac{r_0}{r_{ij}}\right)^{m_a} \exp\left\{m_b\left[-\left(\frac{r_{ij}}{r_c}\right)^{m_c} + \left(\frac{r_0}{r_c}\right)^{m_c}\right]\right\} \qquad (2)$$

This radial dependence of the repulsive potential had been first introduced by Goodwin et al.[21] The parameters (V_{core}, r_0, r_c, m_a, m_b, and m_c) have fixed values for each bond type (see Tables 1 and 2). Finally, the third term, V_{TB}, corresponds to the TB potential which is calculated by

$$V_{TB} = \sum_l n_l \langle \Psi_l | h_{TB} | \Psi_l \rangle + U \sum_l \delta_{n_l,2} \qquad (3)$$

The first contribution in V_{TB} corresponds to the sum of the molecular eigenvalues on all of the molecular states (whose molecular orbitals are labeled $|\Psi_l\rangle$). The number of electrons in the lth molecular state is noted n_l. The eigenstates $|\Psi_l\rangle$ are obtained after diagonalization of the matrix whose h_{TB} Hamiltonian operator is defined by

$$h_{TB} = \sum_{i,\alpha} \epsilon_\alpha^{(i)} |\varphi_\alpha^{(i)}\rangle\langle\varphi_\alpha^{(i)}| + \sum_{i,\alpha} \sum_{j\neq i,\beta} t_{\alpha,\beta}^{(i,j)}(r_{ij}) |\varphi_\alpha^{(i)}\rangle\langle\varphi_\beta^{(j)}| \qquad (4)$$

where $|\varphi_\alpha^{(i)}\rangle$ corresponds to the atomic orbital α centered on the

*i*th atom. For carbons, the 2s and 2p orbitals have been taken into account although only the 1s orbital has been considered for hydrogens. Consequently, for a C_nH_m system, we have to build an $(N \times N)$ matrix, with $N = 4n + m$. It is important to note that the set of atomic orbitals has been taken as an orthogonal basis, i.e., that $\langle\varphi_\alpha^{(i)}|\varphi_\beta^{(j)}\rangle = \delta_{ij}\delta_{\alpha\beta}$.

The off-diagonal elements of the TB Hamiltonian h_{TB}, also called the hopping matrix elements, correspond to the interaction between the atomic orbitals. These elements, noted $t_{\alpha,\beta}^{(i,j)}$, are assumed to follow the same radial dependence as the repulsive part of the potential [see eq 2]. Thus, we have

$$t_{\alpha,\beta}^{(i,j)}(r_{ij}) = t_{\alpha,\beta}^{(i,j)}\left(\frac{r_0}{r_{ij}}\right)^{n_a} \exp\left\{n_b\left[-\left(\frac{r_{ij}}{r_t}\right)^{n_c} + \left(\frac{r_0}{r_t}\right)^{n_c}\right]\right\} \quad (5)$$

The angular part of the hopping matrix elements for the s−p and p−p interactions are calculated following the initial work of Slater.[22] The parameters ($t_{\alpha,\beta}^{(i,j)}$, r_t, n_a, n_b, and n_c) are quoted in Tables 1 and 2 for each bond type.

If the *l*th molecular state is written as $|\Psi_l\rangle = \Sigma_{\alpha,k}\, c_{\alpha,k}^{(l)}|\varphi_\alpha^{(k)}\rangle$, the TB potential energy finally reads

$$V_{TB} = \sum_l n_l \sum_{i,\alpha}\sum_{j,\beta} c_{i,\alpha}^{(l)*}\, c_{j,\beta}^{(l)}\, \langle\varphi_\alpha^{(i)}|h_{TB}|\varphi_\beta^{(j)}\rangle + U\sum_l \delta_{n_l,2} \quad (6)$$

The last term in this expression is an empirical way of taking into account the electron−electron interaction. Because of the positive value of the parameter U (see Table 1), a loss of stability is obtained when two electrons are located on the same molecular orbital. In this context, the evaluation of the minimal potential energy at each time step of the propagation of the system implies the search for the electronic population in the molecular states which minimizes the total energy.

The parameters for the C−H and H−H bonds are reported in Table 1, and the C−C parameters are tabulated in Table 2. Two sets of parameters, previously proposed by Wang et al.[19] [set (I)] and Winn et al.[20] [set (II)], have been used. Note that, in the parametrization of Wang et al.,[19] there is no parameter for the H−H interaction. A new set of parameters developed by us, called set (III), is also presented in Tables 1 and 2. This new parametrization will be discussed later in the paper.

B. Tight-Binding Molecular Dynamics. In the TB scheme, it is possible to propagate the classical equations by calculating analytically the forces acting on each atom. This is done by using the Hellmann−Feynman theorem which allows us to calculate the derivatives of the TB potential with respect to the Cartesian coordinates. The contribution to the force on the *k*th atom coming from V_{TB} is given by

$$F_q^{(k)} = -\frac{\partial}{\partial q_k}\sum_l n_l \langle\Psi_l|h_{TB}|\Psi_l\rangle = -\sum_l n_l \left\langle\Psi_l\left|\frac{\partial h_{TB}}{\partial q_k}\right|\Psi_l\right\rangle \quad (7)$$

with $q \equiv x$, y or z.

By using the decomposition of the molecular states on the atomic basis and the expression of the elements of the hopping matrix, we obtain

$$F_q^{(k)} = -\sum_l n_l \sum_{i,\alpha}\sum_{j,\beta} c_{i,\alpha}^{(l)*}\, c_{j,\beta}^{(l)} \left\langle\varphi_\alpha^{(i)}\left|\frac{\partial h_{TB}}{\partial q_k}\right|\varphi_\beta^{(j)}\right\rangle = -\sum_l n_l \sum_{i,\alpha}\sum_{j\neq i,\beta} c_{i,\alpha}^{(l)*}\, c_{j,\beta}^{(l)} \frac{\partial t_{\alpha,\beta}^{(i,j)}(r_{ij})}{\partial q_k} \quad (8)$$

The numerical integration of the classical equations has been done using the Adams−Moulton predictor−corrector algorithm with a time step equal to 0.15 fs.

Minimum energy structures were found from a quenching procedure which consists of adding a friction force in order to cool the energy of the system. At the end of the quenching trajectories, the atomization energy, the permanent dipole moment, and the equilibrium geometry of the molecule are calculated.

Finally, at the equilibrium geometry, the normal-mode frequencies are obtained using a numerical determination and diagonalization of the Hessian matrix. The Cartesian displacements of the atoms for each normal mode were analyzed in order to fully characterize the set of modes according to their symmetries.

C. Spectral Simulation. The absorption cross-section $\sigma(\omega)$ can be expressed as a function of the absorption line shape $I(\omega)$[23] by

$$\sigma(\omega) = \frac{4\pi^2\omega[1 - e^{-\beta\hbar\omega}]}{3\hbar cn} I(\omega)$$

In this expression, $\hbar$ is the Planck constant, c is the velocity of light, and n is the refractive index of the dielectric medium. The line shape is known to be expressed by the Fourier transform of the classical autocorrelation function $C(t)$ of the dipole moment.

Along a given TB microcanonical trajectory, the charge on each atom can be calculated, and then the dipole moment vector $\boldsymbol{\mu}(t)$ can be easily obtained from

$$\boldsymbol{\mu}(t) = \sum_k e_k \mathbf{r}_k(t) \quad (9)$$

where e_k, the charge of the *k*th atom, is defined by

$$e_k = e_{core}^{(k)} - \sum_l n_l \sum_{i,\alpha}\sum_{j,\beta} c_{i,\alpha}^{(l)*}\, c_{j,\beta}^{(l)} \langle\varphi_\alpha^{(i)} \mid \varphi_\beta^{(j)}\rangle = e_{core}^{(k)} - \sum_l n_l \sum_{i,\alpha} |c_{i,\alpha}^{(l)}|^2 \quad (10)$$

where $e_{core}^{(k)}$ corresponds to the charge of the ionic core of the *k*th atom. To simulate the absorption spectrum, we have to build the autocorrelation function $C(t)$ of the dipole

$$C(t) = \frac{\langle\boldsymbol{\mu}(0).\boldsymbol{\mu}(t)\rangle}{\langle\boldsymbol{\mu}(0).\boldsymbol{\mu}(0)\rangle} = \frac{1}{N}\sum_{i=1}^{N} \boldsymbol{\mu}(t_0^{(i)}).\boldsymbol{\mu}(t + t_0^{(i)}) \quad (11)$$

The total time of each trajectory is 6.144 ps, and the total number of trajectories allowing us to construct the autocorrelation function is $N = 4000$ (10 sets of 400 trajectories). Finally, $I(\omega)$ was obtained from a fast fourier transform (FFT) of the $C(t)$ function.

TABLE 3: Geometric Parameters for the Neutral Naphthalene Molecule (See Numbering of Atoms in Figure 1)[a]

	theoretical results				experimental data	
	set (I)[19]	set (II)[20]	set (III)	Pauzat et al.[11]	Ketkar et al.[32]	Ponomarev[33]
C_1C_1'	1.458	1.432	1.441	1.409	1.412	1.421
C_1C_2	1.471	1.433	1.468	1.421	1.422	1.424
C_2C_3	1.406	1.392	1.374	1.358	1.381	1.377
C_3C_3'	1.447	1.423	1.427	1.417	1.417	1.411
C_2H_2	1.096	1.087	1.099	1.076	1.092	1.095
C_3H_3	1.096	1.088	1.099	1.075	1.092	1.098
$C_2C_1C_1$	118.833	119.632	118.071	118.969	119.5	119.0
$C_2C_1C_1'$	120.777	119.777	121.569	120.778		120.2
$C_3C_2C_1$	120.572	120.774	120.543	120.253		120.5
$H_2C_2C_1$	118.835	120.027	118.224	118.838		117.0
$H_3C_3C_2$	120.473	120.006	120.612	120.253		119.9

[a] Set (III) corresponds to the optimized parameters proposed in this work. Bond distances are expressed in angstroms and angles in degrees.

This classical method allows us to extract spectral information at a given vibrational energy in the molecule. In particular, some spectral features (position and intensity of vibrational bands) as a function of internal energy (or temperature) can be obtained, which appears to be important information in the context of the emission of the PAH in the interstellar medium, as explained in the Introduction.

D. Adiabatic Switching Method. In the classical simulations of the vibrational dynamics of molecules, one general difficulty is the choice of the initial conditions allowing us to mimic the initial quantum vibrational state. One elegant method, namely, adiabatic switching (AS), has been proposed by Johnson[24] which has rediscovered a prior work of Solov'ev.[25] This method is, in fact, linked to the invariance of the classical action variable[26] J_i ($= \oint p_i dq_i$) in an adiabatic transformation of the Hamiltonian.

The semiclassical states will verify the semiclassical condition $J_i = (n_i + (1/2))\hbar$ in which n_i is an integer which corresponds to the quantum number. As a consequence of the invariance of J_i in the adiabatic transformation, the vibrational quantum numbers will also be conserved.

The initial Hamiltonian, noted H_0, has been chosen as the separable harmonic normal mode Hamiltonian. If we call Q_i the ith normal mode and P_i its conjugated momentum, the H_0 Hamiltonian is written as

$$H_0 = \sum_i \left(\frac{P_i^2}{2} + \frac{1}{2}\omega_i^2 Q_i^2 \right) \tag{12}$$

in which ω_i is the pulsation of the ith vibrational normal mode. For this separable Hamiltonian, the semiclassical quantization is direct by using the simple relationships

$$Q_i = \left[\frac{(2n_i + 1)\hbar}{\omega_i} \right]^{1/2} \sin \varphi_i \tag{13}$$

$$P_i = -[(2n_i + 1)\hbar\omega_i]^{1/2} \cos \varphi_i \tag{14}$$

In these relations, φ_i corresponds to the phase (randomly chosen between 0 and 2 π) and n_i is the vibrational quantum number associated to the ith mode.

A slow (adiabatic) transformation is thus initiated between the separable Hamiltonian H_0 and the "real" TB Hamiltonian H_{TB}. This adiabatic evolution is governed by the time-dependent Hamiltonian $H(t)$, expressed as

$$H(t) = g(t)H_{TB} + [1 - g(t)]H_0 \tag{15}$$

If we call T_{AS} the total time of the adiabatic switching, the $g(t)$ function is equal to 0 at $t = 0$ and is equal to 1 at $t = T_{AS}$.

Following the work of Johnson,[24] two different $g(t)$ functions appear as superior; that is, they give a small dispersion of the final energy for a given adiabatic switching time. These two analytic functions are given by

$$g_1(t) = 2\pi\tau + \sin(2\pi\tau) \tag{16}$$

and

$$g_2(t) = -\tau\{[(20\tau - 70)\tau + 84]\tau - 35\} \tag{17}$$

where $\tau = (t/T_{AS})$.

Previous works[27,28] have shown that T_{AS} has to be equal to about 100 T_{max} in which T_{max} corresponds to the largest period of the normal modes.

The numerical integration of the Hamilton's equations has been done following the same procedure as explained before, i.e., by using the Adams−Moulton predictor−corrector algorithm. To transform the normal mode coordinates into Cartesian coordinates, the orthogonal matrix (calculated at the minimum energy configuration) that connects normal modes to the mass-weighted Cartesian coordinates has been used.

It has to be noted that the adiabatic switching method has been already used to calculate the eigenvalues for triatomic molecules,[27,29,30] six-dimensional systems,[29] and also the CH_4 molecule.[31] To our knowledge, it is the first time that this method is used for such a large polyatomic molecule.

III. Results and Discussion

A. Bond Lengths and Harmonic Normal-Mode Frequencies at Equilibrium Geometry. We present first the results obtained on the equilibrium geometry for the neutral $C_{10}H_8$ naphthalene molecule with the two sets of TB parameters that were found in the literature. These results, reported in Table 3, have been compared with those of the ab initio calculation (UHF, 6-31G* basis) done by Pauzat et al.[11] Some experimental values are also given in the two last columns of this Table. The labels used for numbering the C and H atoms follow the paper of Pauzat et al.,[11] and they are recalled in Figure 1. Set (II) clearly gives a better agreement with the ab initio values[11] but also with the experimental values. Set (I) tends to overestimate all of the C−C bond lengths. This tendency can also be seen in the initial work of Wang et al.[19] in which the C−C bond length for the benzene molecule was also overestimated. It is remarkable that the two sets of parameters perfectly reproduce the C−H experimental equilibrium distances.

The results for harmonic normal-mode frequency analyses obtained from the two sets of parameters are given in Table 4 for comparison with the ab initio values of Pauzat et al.[11]

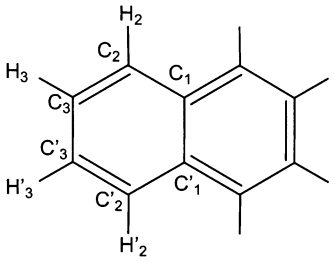

Figure 1. Definition of geometric parameters of the naphthalene molecule.

TABLE 4: Normal Mode Harmonic Frequencies for the IR Active Modes of the Neutral Naphthalene Molecule[a]

				Pauzat et al. [ref 11]		Langhoff [ref 12]	
D_{2h}	set (I) [ref 19]	set (II) [ref 20]	set (III) this work	without scaling factor	with scaling factor	without scaling factor	with scaling factor
b_{3u}	177	133	186	188	172	179	172
b_{3u}	477	363	507	535	485	501	480
b_{3u}	858	573	862	887	791	823	788
b_{3u}	1086	918	1119	1098	977	1006	964
b_{1u}	386	297	386	389	364	376	361
b_{1u}	861	714	892	859	781	832	797
b_{1u}	1271	1035	1258	1245	1130	1182	1132
b_{1u}	1447	1199	1413	1390	1261	1326	1270
b_{1u}	1620	1373	1603	1543	1364	1461	1400
b_{1u}	1749	1719	1707	1806	1654	1663	1593
b_{1u}	3313	3047	3125	3353	3047	3177	3044
b_{1u}	3314	3067	3140	3374	3071	3197	3063
b_{2u}	645	523	683	674	596	660	632
b_{2u}	1196	1011	1164	1075	988	1054	1010
b_{2u}	1317	1039	1200	1193	1091	1221	1170
b_{2u}	1365	1218	1338	1311	1165	1262	1209
b_{2u}	1464	1489	1428	1476	1321	1418	1358
b_{2u}	1706	1617	1664	1683	1539	1574	1508
b_{2u}	3312	3037	3126	3355	3052	3179	3045
b_{2u}	3318	3063	3136	3385	3083	3211	3077

[a] Frequencies are expressed in cm^{-1}.

(Hartree−Fock with a 6-31G* basis) and Langhoff[12] (DFT calculation using the 4-31G basis and the B3LYP functional). Some strong differences between the values issued from set (I) and from set (II) are evidenced, with the frequencies obtained with set (II) being systematically smaller than those obtained with set (I). It is important to note that, in the ab initio calculations, a scaling factor has been applied in order to improve the agreement with the experimental data. In Table 4, the unscaled and the scaled frequencies are reported. Langhoff[12] applied a constant scaling factor (=0.958), whereas different scaling factors have been applied by Pauzat et al.[11] depending on the nature of the vibrational modes (stretching, in-plane bending or out-plane bending). The values of the TB normal-mode frequencies obtained from set (I) and the unscaled ab initio frequencies of Pauzat et al.[11] and of Langhoff[12] are approximately in the same range with an average relative difference of 3.9% and 5.8%, respectively, whereas set (II) tends to give values lower than the theoretical unscaled frequencies.

As the anharmonicity of the PES is sometimes invoked to explain the scaling factors, the anharmonicity within the two TB parametrizations [sets (I) and (II)] has been analyzed first. This is done by using the AS method to evaluate the energies of the classical system corresponding to well-defined states of the quantum system.

B. Analysis of the Anharmonicity and Optimization of the Potential. In a first step, we prepared the system at the zero-point energy (ZPE). The AS procedure has been tested for set

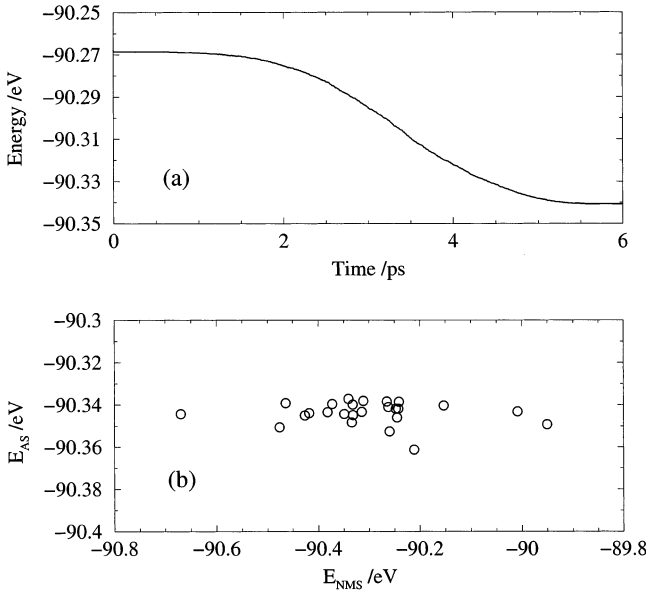

Figure 2. Adiabatic Switching procedure with $g_2(t)$ and $T = 6$ ps in the case of set (I): (a) Energy as a function of time during a typical adiabatic switching trajectory and (b) zero-point energy of the naphthalene obtained from the normal mode sampling procedure (E_{NMS}) and from the adiabatic switching procedure (E_{AS}).

(I) by using both functions [see eqs 16 and 17] transforming the normal mode separable Hamiltonian into the TB Hamiltonian. The comparison of the dispersion of the final energy has shown that the $g_2(t)$ function gives slightly better results than the $g_1(t)$ one, as reported by Johnson[24] in the case of a model calculation of two coupled harmonic oscillators. Consequently, only the $g_2(t)$ function has been used further in this work.

The typical evolution of the zero point energy in one AS trajectory is shown in Figure 2a. It appears that the energy of the system evolves very smoothly as a function of the time. However, as the final energy can be slightly dependent on the initial phases φ_i (because of the finite time of the adiabatic switching trajectory), we have run 25 AS trajectories to obtain confident results for the final zero point energy. In Figure 2b, the AS final energies are compared with the energy obtained from a normal mode sampling (NMS), which consists of taking the semiclassical initial conditions for the H_0 separable Hamiltonian as the initial conditions for the TB Hamiltonian [see eqs 13 and 14]. Figure 2b directly shows that the NMS procedure induces a strong dispersion of the zero-point energy because of the anharmonicity of the potential energy surface in the energy range around the ground vibrational state. On the other hand, the AS procedure gives a very small energy dispersion of the final energy (about 0.005 eV). This dispersion gives an upper limit for the uncertainty on the final energy. In summary, the average value of the zero-point energy with respect to the bottom of the potential well is now $E_{ZPE}^{(anharm.)} = 4.206 \pm 0.005$ eV to be compared with the harmonic value $E_{ZPE}^{(harm.)} = 4.280$ eV.

Following the same scheme, it has been possible to calculate the energies of specific vibrational states within set (I). The anharmonic vibrational frequencies are thus derived by subtracting the above ZPE value. As an illustration, we consider the frequencies for modes 1 and 9 (the modes are numbered from the largest to the smallest frequencies). The anharmonic values were found at $\omega_1 = 3178$ cm^{-1} and $\omega_9 = 1702$ cm^{-1} to be compared with the harmonic frequencies found at $\omega_1 = 3318$ cm^{-1} and $\omega_9 = 1749$ cm^{-1}(see first column of Table 4). This relatively strong anharmonicity was also observed using set (II). As a consequence, because the normal modes extracted from

TABLE 5: Comparison of the Anharmonic Frequencies of IR Active Modes with the Experimental Frequencies Measured in Rare Gas Matrices for the Neutral Naphathalene Molecule[a]

D_{2h}	anharmonic frequencies	Hudgins et al.[10]	Szczepanski et al.[9]	Krainov[34]
b_{3u}	169			176
b_{3u}	484	472−483 (0.15)		476
b_{3u}	823	780−790 (1.0)	783, 788 (1.00)	782
b_{3u}	1057	956−963 (0.02)	958, 960 (0.03)	958
b_{1u}	379			359
b_{1u}	863			753
b_{1u}	1202	1127−1142 (0.07)	1129, 1131 (0.05)	1125
b_{1u}	1355	1267−1275 (0.07)	1269, 1272 (0.05)	1265
b_{1u}	1532	1388−1395 (0.06)	1391, 1394 (0.05)	1389
b_{1u}	1645	1599−1604 (0.04)	1601 (0.05)	1595
b_{1u}	2960			3058
b_{1u}	2976	3050−3071 (0.21)	3028−3112 (0.37)	3065
b_{2u}	653	617−622 (0.04)		618
b_{2u}	1108	1009−1018 (0.07)	1012, 1016 (0.06)	1008
b_{2u}	1145			1138
b_{2u}	1250	1209−1216 (0.03)	1212, 1214 (0.02)	1209
b_{2u}	1371	1360−1363 (0.02)	1361 (0.02)	1361
b_{2u}	1589	1506−1520 (0.12)	1513, 1515 (0.07)	1506
b_{2u}	2976			3027
b_{2u}	2984	3071−3083 (0.09)		3090

[a] Only frequencies given by our parametrization [set (III)] are reported here. The numbers in parentheses correspond to relative intensities normalized to the most intense band near 800 cm^{-1}.

set (II) are quasi systematically lower than the scaled ab initio and the experimental values and because the situation is made worse due to the anharmonicity, it appears that set (I) gives a better reproduction of the vibrational frequencies.

However, as discussed previously, the equilibrium geometry (especially the C−C distances) suffers from some defects when calculated using the set (I) [see Table 3]. For that reason, we have built a new parametrization, called set (III), which we consider to be optimally adapted for the aromatic molecules. These new parameters are tabulated in Tables 1 and 2. Set (III) is very close to set (I) in order not to alter much the physical significance of the parameters. It has to be noted that the H−H interaction parameters of set (II) have been conserved because the H−H interaction was not considered in set (I). This H−H interaction has no effect on the properties extracted from the low energy behavior of the PAH molecules. In fact, this interaction has been included in order to allow future simulations of the dissociation of the PAH molecules in which the H_2 molecule may be a fragmentation product.

The geometry is now in better agreement with the experimental data as it can be seen in Table 3, especially for the C−C bond length. The major discrepancy is always the C_1C_2 distance, but the other C−C bonds have been shrunk with respect to set (I). With this new parametrization, the C−H distances appear to be in very good agreement with the experimental data. The new harmonic normal-mode frequencies are reported in Table 4. The C−C stretching frequencies (around 1600 cm^{-1}) and the in-plane C−H bending frequencies (around 1200 cm^{-1}) are now slightly lower than in set (I), as expected. To make a valuable comparison between the experimental frequencies and the frequencies obtained with this new parametrization, we have run systematically AS trajectories in order to get the exact anharmonic frequencies of all of the IR active modes using set (III).

The zero-point energy is now equal to 4.100 ± 0.003 eV (to be compared with the harmonic value of 4.174 eV). The anharmonic IR active frequencies are reported in Table 5 and can be directly compared to the experimental data for the neutral

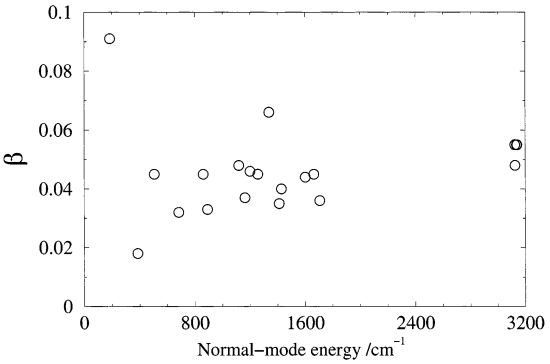

Figure 3. Analysis of the anharmonicity for all the IR active modes from the value of the parameter β (see text).

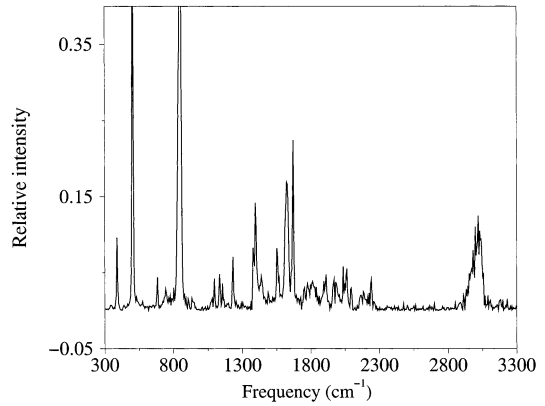

Figure 4. IR absorption spectrum calculated for the naphthalene molecule in its ground vibrational state.

naphthalene trapped in a cold, solid rare gas matrix, obtained by Szczepanski et al.[9] and Hudgins et al.[10] For the C−H stretching modes (around 3050 cm^{-1}), the calculation underestimated the experimental values by about 80 cm^{-1}, which corresponds to about 3% error. For the C−C stretching modes also (around 1500−1600 cm^{-1}), the calculated frequencies are slightly larger than the experimental values by about 3−5%. For the C−C in-plane and C−H out-of-plane bending modes (1200 and 800 cm^{-1}, respectively), the energy differences remain smaller than 50 cm^{-1}. Consequently, an overall quite good agreement is now obtained.

To summarize the importance of the anharmonicity of the PES, we have reported in Figure 3 the values of β ($= (E^{(\text{harm.})} - E^{(\text{anharm.})}/E^{(\text{harm.})})$) for all of these modes. The order of magnitude of β is 0.04, and no mode-specific anharmonic effects can be demonstrated. It is interesting to note that the anharmonicity coefficient ($1 - \beta$) is almost equal to the scaling factor used by Langhoff[12] to reproduce in the optimum way the experimental frequencies from the DFT calculation.

C. Vibrational Spectrum. The values of the normal-mode frequencies derived from set (III), taking into account the anharmonic character of the PES thanks to the AS procedure, have been given in section III.B. In this part, we present the full infrared spectrum generated from the dipole autocorrelation function. Classical trajectories were run in the microcanonical ensemble with the initial conditions corresponding to the neutral naphthalene molecule in its ground vibrational state. The calculated vibrational spectrum is displayed in Figure 4. The calculated relative integrated intensities have also been plotted in Figure 5a for comparison with the experimental results reported by Hudgins et al.(Figure 5b). The mean frequencies

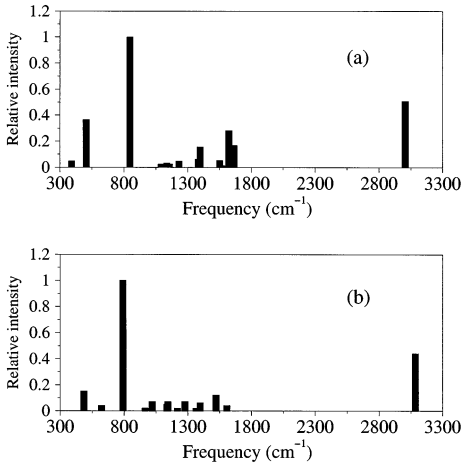

Figure 5. Comparison between the integrated intensities in the IR absorption spectrum of the neutral naphthalene derived from (a) the present theoretical work (see Figure 4) and (b) the experimental work of Hudgins et al.[10]

have been integrated by the features which are apparent in Figure 4, which may include contributions from several vibrational modes.

We can first note that the overall pattern of the experimental spectrum is well reproduced. Indeed, our theoretical spectrum is dominated by one strong peak at $\omega = 846$ cm^{-1} (C−H out-of-plane bending mode) as in the experimental case (the most intense peak is observed at $\omega = 783$ cm $^{-1}$). Moreover, the C−H stretch band is the second most intense band in the experimental spectrum[10] as well as in our result. Two vibrational bands were experimentally found at $\omega' = 3065$ cm^{-1} and $\omega'' = 3078$ cm^{-1}, with relative integrated intensities (with respect to the most intense band) respectively equal to 0.21 (integrated between 3050 and 3071 cm^{-1}) and 0.09 (integrated between 3071 and 3083 cm^{-1}). Hudgins et al. also quoted an overall integrated intensity of two these bands equal to 0.44, in good agreement with the value given by Szczepanski et al.: the integrated intensity (between 3028 and 3112 cm^{-1}) is equal to 0.37. These values are in good agreement with the relative integrated intensity obtained from our theoretical spectrum, which is equal to 0.50. It can also be compared with the value 0.66 measured by Joblin et al.[35] in the gas phase (at about 400 K). Finally, it can to be noted that the HF and DFT calculations largely overestimate the integrated intensities of the C−H stretching modes when compared to the experiment. Langhoff has found a value as large as 1.44 and invoked a matrix perturbation to explain such a discrepancy.

Following the experimental work of Hudgins et al.,[10] the next most intense peak is observed at $\omega = 474$ cm^{-1} (with a relative intensity equal to 0.15). In our theoretical spectrum, this peak is found at $\omega = 505$ cm^{-1} with a relative integrated intensity equal to 0.37. This band corresponds to a C−C out-of-plane bending mode. It was out of the accessible frequency window in the work of Szczepanski et al.[9]

Smaller peaks are also present in our spectrum within the spectral range 1300−1600 cm^{-1} (C−C stretching modes). Their relative integrated intensities are larger than the experimental results. Others peaks, in the 1000−1200 cm^{-1} energy range (C−H in-plane bending modes), show a satisfactory agreement with experimental intensities (in the order of 2−5%). Hence, the global features of the experimental data appear to be quite well reproduced by our model as can be clearly seen by comparing parts a and b of Figure 5.

IV. Conclusion and Perspectives

In summary, a new theoretical approach to investigate the vibrational dynamics of highly excited polycyclic aromatic hydrocarbon derivatives has been coined, which is reported in this paper. It combines a tight-binding potential to evaluate the electronic energy and wave functions at any particular configuration of the hydrocarbonated system of interest, classical trajectories to analyze the vibrational motion, and an adiabatic switching procedure to prepare the classical system in initial conditions that mimic any vibrational quantum state of interest. An optimized parametrization of the tight-binding potential for aromatic systems has been proposed. This tool has allowed a detailed study of the normal-mode frequencies and the anharmonic effects in the neutral naphthalene molecule, taken as a model system of larger PAHs and derivatives containing about 10 eV of internal energy, supposed to be present in interstellar space and responsible for the observed strong IR emission fingerprints.

The IR absorption spectrum of the naphthalene molecule in its ground quantum state has been simulated thanks to a spectral density approach and found to be in good agreement with the experimental spectrum in low-temperature rare gas matrixes. In particular, the relative intensities of the various bands are well reproduced.

The same tool can be used to investigate the sensitivity of the IR band positions and intensities to astrophysically important parameters. These include internal energy (or photon energy of the starlight), ionization state, or hydrogenation state, as well as their evolution with the PAH size and/or structure (catacondensed/pericondensed), up to large sizes for which present ab initio methods become very difficult. Such work is presently in progress: it has already been shown that the main effects revealed by costly theoretical means are reproduced. It will be the subject of forthcoming publications. Results will ultimately be included in astrophysical models of the emission from specific objects in space.

References and Notes

(1) Léger, A.; Puget, J. L. *Astron. Astrophys.* **1984**, *137*, L5.
(2) Léger, A.; d'Hendecourt, L. *Astron. Astrophys.* **1985**, *146*, 81.
(3) Allamandola, L. J.; Tielens, A. G. G. M.; Baker, J. R. *Astrophys. J.* **1985**, *290*, L25.
(4) Van der Zwet, G. P.; Allamandola, L. J. *Astron. Astrophys.* **1985**, *146*, 77.
(5) Crawford, M. K.; Tielens, A. G. G. M.; Allamandola, L. J. *Astrophys. J.* **1985**, *293*, L45.
(6) Russell, R. W.; Soifer, B. T.; Merrill, K. M. *Astrophys. J.* **1977**, *213*, 66.
(7) Russell, R. W.; Soifer, B. T.; Willner, S. P. *Astrophys. J.* **1977**, *217*, L149. Russell, R. W.; Soifer, B. T.; Willner, S. P. *Astrophys. J.* **1977**, *220*, 568.
(8) Sellgren, K.; *Astrophys. J.* **1984**, *277*, 623.
(9) Szczepanski, J.; Vala, M. *Astrophys. J.* **1993**, *414*, 179.
(10) Hudgins, D. M.; Sandford, S. A.; Allamandola, L. J. *J. Phys. Chem.* **1994**, *98*, 4243.
(11) Pauzat, F.; Talbi, D.; Miller, M. D.; DeFrees, D. J.; Ellinger, Y. *J. Phys. Chem.* **1992**, *96*, 7882.
(12) Langhoff, S. R. *J. Phys. Chem.* **1996**, *100*, 2819.
(13) Martin, J. M. L.; El-Yazal, J.; François, J. P. *J. Phys. Chem.* **1996**, *100*, 15358.
(14) Car, R.; Parrinello, M. *Phys. Rev. Lett.* **1985**, *55*, 2471.
(15) Wang, C. Z.; Chan, C. T.; Ho, K. M. *Phys. Rev. B* **1989**, *39*, 8592.
(16) Wang, C. Z.; Chan, C. T.; Ho, K. M. *Phys. Rev. Lett.* **1991**, *66*, 189.
(17) Khan, F. S.; Broughton, J. Q. *Phys. Rev. B* **1989**, *39*, 3688.
(18) Yu, J.; Kalia, R. K.; Vashishta, P. *Phys. Rev. B* **1994**, *49*, 5008.
(19) Wang, Y.; Mak, C. H. *Chem. Phys. Lett.* **1995**, *235*, 37.
(20) Winn, M. D.; Rassinger, M.; Hafner, J. *Phys. Rev. B* **1997**, *55*, 5364.
(21) Goodwin, L.; Skinner, A. J.; Pettifor, D. G. *Europhys. Lett.* **1989**, *9*, 701.

(22) Slater, J. C.; Koster, G. F. *Phys. Rev. A* **1954**, *94*, 1498.
(23) McQuarrie, D. A.; *Statistical Mechanics*; Harper and Row: New York, 1976.
(24) Johnson, B. R. *J. Chem. Phys.* **1985**, *83*, 1204.
(25) Solov'ev, E. A. *Sov. Phys. JETP* **1978**, *48*, 635.
(26) Landau, L. D.; Lifshitz, E. M. *Mechanics* Addison-Wesley: Reading, MA, 1980).
(27) Johnson, B. R. *J. Chem. Phys.* **1987**, *86*, 1445.
(28) Reinhardt, W. *J. Mol. Struct.* **1990**, *223*, 157.
(29) Sun, Q.; Bowman, J. M.; Gozdy, B. *J. Chem. Phys.* **1988**, *89*, 3214.
(30) Aubanel, E. E.; Wardlaw, D. M. *J. Chem. Phys.* **1988**, *88*, 495.
(31) Huang, J.; Valentini, J. J.; Muckerman, J. T. *J. Chem. Phys.* **1995**, *102*, 5695.
(32) Ketkar, N.; Fink, M. *J. Mol. Struct.* **1981**, *77*, 139.
(33) Ponomarev, V. I.; Filipenko, O. S.; Atovmyan, L. O. *Kristallografiya* **1976**, *21*, 392.
(34) Krainov, E. P. *Opt. Spektrosk.* **1964**, *16*, 415 and 763.
(35) Joblin, C.; private communication.